The yeast arrestin-related protein Bul1 is a novel actor of glucose-induced endocytosis

Junie Hovsepian[a,†], Véronique Albanèse[a,†], Michel Becuwe[a,‡], Vasyl Ivashov[b], David Teis[b], and Sébastien Léon[a,*]

[a]Institut Jacques Monod, UMR 7592 Centre National de la Recherche Scientifique/Université Paris-Diderot, Sorbonne Paris Cité, 75205 Paris, France; [b]Division of Cell Biology, Biocenter, Medical University of Innsbruck, 6020 Innsbruck, Austria

ABSTRACT **Yeast cells have a remarkable ability to adapt to nutritional changes in their environment. During adaptation, nutrient-signaling pathways drive the selective endocytosis of nutrient transporters present at the cell surface. A current challenge is to understand the mechanistic basis of this regulation. Transporter endocytosis is triggered by their ubiquitylation, which involves the ubiquitin ligase Rsp5 and its adaptors of the arrestin-related family (ART). This step is highly regulated by nutrient availability. For instance, the monocarboxylate transporter Jen1 is ubiquitylated, endocytosed, and degraded upon exposure to glucose. The ART protein Rod1 is required for this overall process; yet Rod1 rather controls Jen1 trafficking later in the endocytic pathway and is almost dispensable for Jen1 internalization. Thus, how glucose triggers Jen1 internalization remains unclear. We report that another ART named Bul1, but not its paralogue Bul2, contributes to Jen1 internalization. Bul1 responds to glucose availability, and preferentially acts at the plasma membrane for Jen1 internalization. Thus, multiple ARTs can act sequentially along the endocytic pathway to control transporter homeostasis. Moreover, Bul1 is in charge of Jen1 endocytosis after cycloheximide treatment, suggesting that the functional redundancy of ARTs may be explained by their ability to interact with multiple cargoes in various conditions.**

Monitoring Editor
Sandra Lemmon
University of Miami

Received: Jul 26, 2017
Revised: Feb 26, 2018
Accepted: Feb 27, 2018

INTRODUCTION

Endocytosis contributes to plasma membrane homeostasis and is critical for cellular adaptation. Whereas the molecular mechanisms driving endocytosis of ligand-bound receptors (e.g., EGF [epidermal growth factor] receptor) are relatively well characterized (Sigismund *et al.*, 2012), less is known about the endocytosis of nutrient transporters. Transporter abundance regulates the uptake capacity of cells and their ability to proliferate, and altering the regulation of uptake systems in cancer cells is a strategy for therapeutic interventions (McCracken and Edinger, 2013). Thus, a deeper understanding of the physiological regulation of nutrient transporters is needed.

The yeast *Saccharomyces cerevisiae* is an ideal model system to study how eukaryotic cells cope with changes in extracellular nutrients (Broach, 2012). These changes modify transcriptional programs to allow a rapid metabolic rewiring; they also reconfigure nutrient transport systems present at the plasma membrane through selective endocytosis (Haguenauer-Tsapis and André, 2004). A current challenge is to understand how nutrient-signaling pathways drive the endocytosis of specific nutrient transporters.

Transporter ubiquitylation triggers their endocytosis (MacGurn *et al.*, 2012). This reaction is performed by the Nedd4-like E3 ubiquitin ligase Rsp5 whose metazoan homologues also contribute to endocytosis (Hein *et al.*, 1995; Galan *et al.*, 1996; Rotin and Kumar, 2009). The discovery of Rsp5 adaptor proteins of the arrestin-related family (ARTs: arrestin-related trafficking adaptors) improved our understanding of the regulation of this step (reviewed in Becuwe *et al.*, 2012a; Piper *et al.*, 2014). ARTs promote Rsp5 association with transporters to facilitate their ubiquitylation, but also warrant the timeliness of this interaction with respect to environmental cues

This article was published online ahead of print in MBoC in Press (http://www.molbiolcell.org/cgi/doi/10.1091/mbc.E17-07-0466) on March 5, 2018.

†These authors contributed equally to this work.

‡Present address: Department of Genetics and Complex Diseases, Harvard School of Public Health, Boston, MA 02115.

*Address correspondence to: Sébastien Léon (sebastien.leon@ijm.fr).

Abbreviations used: ART, arrestin-related trafficking adaptor; CHX, cycloheximide; PHFAPP1, pleckstrin-homology domain of four-phosphate-adaptor protein 1; SC, synthetic complete medium; TGN, *trans*-Golgi network.

(Lin *et al.*, 2008; Nikko *et al.*, 2008; Nikko and Pelham, 2009). ARTs are targets of nutrient-signaling pathways, so they serve as nutrient-responsive conditional adaptors when cells undergo nutritional challenges (O'Donnell *et al.*, 2010, 2013, 2015; MacGurn *et al.*, 2011; Becuwe *et al.*, 2012b; Merhi and André, 2012; Llopis-Torregrosa *et al.*, 2016; Hovsepian *et al.*, 2017; Talaia *et al.*, 2017). In other situations, such as when endocytosis is elicited by heat shock, oxidative stress, or substrate translocation, ARTs remain central to this regulation but it is not clear whether and/or how their activity is regulated (Nikko *et al.*, 2008; Gournas *et al.*, 2010; Hatakeyama *et al.*, 2010; Karachaliou *et al.*, 2013; Keener and Babst, 2013; Zhao *et al.*, 2013; Crapeau *et al.*, 2014; Ghaddar *et al.*, 2014; Guiney *et al.*, 2016). Finally, ARTs regulate the endocytosis of the G protein–coupled receptor Ste2 (Alvaro *et al.*, 2014, 2016).

ART regulation has particularly been studied during variations in nitrogen or carbon supplies (O'Donnell *et al.*, 2010, 2015; MacGurn *et al.*, 2011; Becuwe *et al.*, 2012b; Merhi and André, 2012; Llopis-Torregrosa *et al.*, 2016; Hovsepian *et al.*, 2017). Rod1 is a glucose-responsive ART required for the glucose-induced degradation of transporters (Nikko and Pelham, 2009; Becuwe *et al.*, 2012b; Becuwe and Leon, 2014; Llopis-Torregrosa *et al.*, 2016). Rod1 is phosphoinhibited by the yeast AMPK orthologue Snf1, which is active in the absence of glucose (Shinoda and Kikuchi, 2007; Becuwe *et al.*, 2012b; O'Donnell *et al.*, 2015; Llopis-Torregrosa *et al.*, 2016). Upon glucose exposure, Rod1 is dephosphorylated in a protein phosphatase 1 (PP1)–dependent manner, and then ubiquitylated by Rsp5, both of which are required for Rod1 activity in endocytosis. Thus, ARTs posttranslational modifications relay the nutrient status of the cell to transporter endocytosis.

ARTs are considered to act mainly for cargo ubiquitylation at the plasma membrane. Live-cell imaging of the glycerol transporter Stl1 after glucose treatment revealed a block in its internalization in a *rod1*Δ strain, suggesting that Rod1 acts at the plasma membrane. Yet Rod1 is almost dispensable for the internalization of another cargo, the lactate transporter Jen1 (Becuwe and Leon, 2014), despite being required for the overall process of its glucose-induced degradation (Becuwe *et al.*, 2012b). In *rod1*Δ cells, Jen1 internalization is slowed down but Jen1 recycles back to the plasma membrane, because Rod1 additionally acts in the postendocytic sorting of Jen1. After internalization, Jen1 is retrograde-trafficked to the *trans*-Golgi network (TGN), where Rod1 dynamically localizes after its glucose-induced activation. Upon sustained glucose exposure, Rod1 promotes Jen1 ubiquitylation by Rsp5 at the TGN, leading to its vacuolar targeting through the ubiquitin-binding, TGN-localized clathrin adaptors Gga1/Gga2. Thus, Rod1 primarily promotes postendocytic Jen1 ubiquitylation. However, how Jen1 is ubiquitylated at the plasma membrane remains incompletely defined.

In this study, we show that the ART-related protein Bul1, but not its paralogue Bul2, is a novel glucose-regulated arrestin-like protein and the missing actor involved in Jen1 internalization in response to glucose. Through this example, we provide evidence that several ARTs can sequentially act on transporters along the endocytic pathway. We propose that different metabolic signals with common signaling pathways favor ectopic ART activation, giving rise to an apparent functional redundancy.

RESULTS AND DISCUSSION

Bul1 functionally assists Rod1 in the glucose-induced endocytosis of the lactate transporter Jen1 and acts primarily at the plasma membrane

In *rod1*Δ cells, Jen1 internalization was delayed but still partially occurred, suggesting the involvement of (an)other adaptor(s) for the glucose-induced internalization of Jen1. Moreover, Jen1 internalization was also observed in a mutant lacking nine arrestin genes, suggesting the involvement of other adaptors (Becuwe and Leon, 2014).

Bul1 and Bul2 are regulators of Gap1 (general amino acid permease) trafficking (Helliwell *et al.*, 2001; Soetens *et al.*, 2001; Risinger and Kaiser, 2008). They act as Rsp5 adaptor proteins (Merhi and André, 2012), sometimes redundantly with ARTs (Nikko and Pelham, 2009; Crapeau *et al.*, 2014) and may share structural features with them (Nikko and Pelham, 2009). We thus considered the possible contribution of Bul1 and Bul2 in Jen1 trafficking.

In WT cells, Jen1-GFP internalization in endosomes is observed as early as 5 min after glucose treatment as previously described (Becuwe and Leon, 2014), and is followed by the vacuolar delivery of Jen1-GFP within 60 min (Figure 1A). It is noteworthy that glucose also represses *JEN1* transcription and promotes the degradation of the corresponding transcripts (Lodi *et al.*, 2002; Chambers *et al.*, 2004; Mota *et al.*, 2014), allowing one to observe the trafficking of preexisting Jen1 in the absence of neosynthesis. As reported, Jen1-GFP internalization still occurred in *rod1*Δ cells, with the persistence of a signal at the plasma membrane and partial targeting to the vacuole at late time points (Figure 1A; Becuwe and Leon, 2014). Strikingly, the deletion of *BUL1* in the *rod1*Δ background almost completely abolished Jen1-GFP internalization (Figure 1A). Bul1 and Bul2 share many functions (Helliwell *et al.*, 2001; Soetens *et al.*, 2001; Abe and Iida, 2003; Pizzirusso and Chang, 2004; Liu *et al.*, 2007; Nikko and Pelham, 2009; Merhi and André, 2012; Crapeau *et al.*, 2014; Villers *et al.*, 2017), yet *BUL2* deletion had no effect on Jen1 sorting (Figure 1, A and B), indicating that Bul1 alone is responsible for the "remnant internalization" reported earlier in the *rod1*Δ mutant (Becuwe and Leon, 2014). Jen1-GFP trafficking was not altered in the single *bul1*Δ mutant, confirming that Rod1 remains the major ART for the glucose-induced endocytosis of Jen1 (Figure 1C).

To precisely place the action of Bul1, we used the fact that Jen1 vacuolar targeting is abolished in a strain lacking Vps52, a subunit of the VFT tethering complex (Conibear and Stevens, 2000; Siniossoglou and Pelham, 2001) in which the endosome-to-TGN retrograde pathway is disrupted (Figure 1D). In *vps52*Δ, Jen1 accumulates in endosomal structures (Figure 1E; Becuwe and Leon, 2014) that did not colocalize with the TGN or the vacuole (Supplemental Figure S1). Of note, these structures originated from the plasma membrane, and not from intracellular compartments, as judged by the inhibitory effect of latrunculin A (an actin polymerization inhibitor and potent inhibitor of endocytosis) on their appearance (Figure 1, E and F). The additional deletion of *ROD1* increased Jen1 localization to the plasma membrane, but did not fully prevent this intracellular accumulation, confirming that internalization still partially occurs in the absence of Rod1 (Figure 1, E and F). In the triple *vps52*Δ *rod1*Δ *bul1*Δ mutant, Jen1 internalization was more severely compromised as Jen1 further accumulated at the plasma membrane (Figure 1, E and F). Therefore, Bul1 promotes Jen1 internalization.

Bul1 is responsible for the residual ubiquitylation and degradation of Jen1 observed in the *rod1*Δ strain

Jen1-GFP was degraded to comparable levels in WT and *bul1*Δ cells after 60 min glucose treatment, but it was partially protected from degradation in the single *rod1*Δ mutant and was almost not degraded in the *rod1*Δ *bul1*Δ mutant (Figure 2, A and B). Bul1 may thus act as an "alternative adaptor" when Rod1 is absent. Earlier studies showed that Jen1 ubiquitylation is readily detectable on total protein extracts, causing a decreased electrophoretic mobility of a fraction of Jen1 (Paiva *et al.*, 2009; Becuwe *et al.*, 2012b;

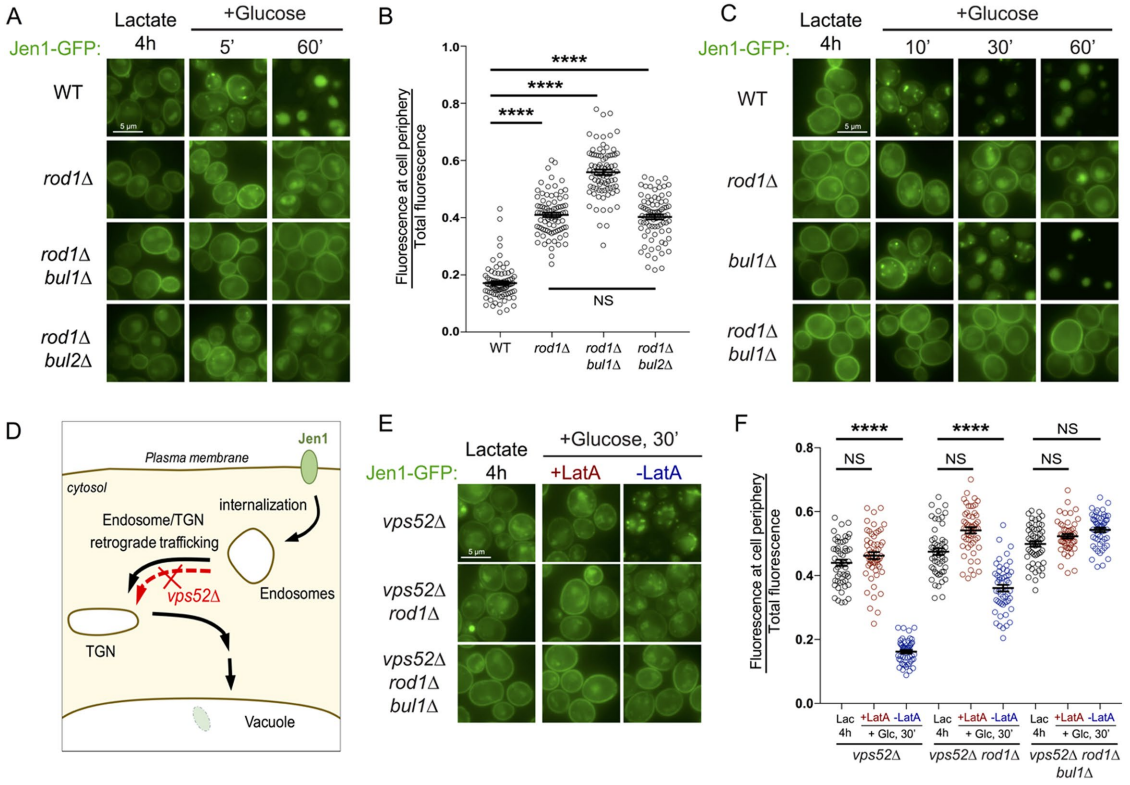

FIGURE 1: Bul1 assists Rod1 in the glucose-induced endocytosis of Jen1, and acts primarily at the plasma membrane. (A) Localization of Jen1-GFP in WT, *rod1*Δ, *rod1*Δ *bul1*Δ, and *rod1*Δ *bul2*Δ cells after 4 h growth in lactate medium (Jen1 induction) and at various times after the addition of glucose. (B) From the experiment presented in A, quantification of the ratio of fluorescence at the cell periphery over total fluorescence at 60 min after glucose treatment (see *Materials and Methods*). (C) Localization of Jen1-GFP in WT, *rod1*Δ, bul1Δ, and *rod1*Δ *bul1*Δ cells after 4 h growth in lactate medium and after glucose treatment. (D) Model of Jen1 trafficking after internalization. The deletion of *VPS52* abrogates the vacuolar targeting of Jen1. (E) Localization of Jen1-GFP in *vps52*Δ, *vps52*Δ *rod1*Δ, and *vps52*Δ *rod1*Δ *bul1*Δ cells grown in the indicated conditions. LatA: latrunculin A. (F) From the experiment presented in E, quantification of the ratio of fluorescence at the cell periphery over total fluorescence at 30 min after glucose treatment.

Becuwe and Leon, 2014). The absence of this shift in the *rod1*Δ *bul1*Δ mutant suggested a defective ubiquitylation in this strain (Figure 2, A–C). Jen1-GFP was immunopurified in denaturing conditions 10 min after glucose treatment, and Jen1-GFP ubiquitylation was compared in WT, *rod1*Δ, and *rod1*Δ *bul1*Δ cells (Figure 2D). Jen1 ubiquitylation was decreased but not fully abolished in *rod1*Δ cells, as reported earlier (Becuwe *et al.*, 2012b). The additional deletion of *BUL1* further impeded Jen1 ubiquitylation, showing that Bul1 is able to sustain a certain level of Jen1 ubiquitylation.

Expression of a TGN-localized version of Rod1 leads to an increased dependency toward the function of Bul1 for Jen1 degradation

We constructed a TGN-targeted version of Rod1 by fusing it to the PH (pleckstrin homology) domain of the human protein FAPP1 (four-phosphate-adaptor protein 1), which interacts with both the TGN-localized PI(4)P and Arf1 (Dowler *et al.*, 2000; He *et al.*, 2011). A PH^{FAPP1}-GFP fusion localizes to the TGN in yeast (Levine and Munro, 2002) and so did Rod1-PH^{FAPP1}-GFP (as defined by the *trans*-Golgi marker Sec7-mCherry:; Franzusoff *et al.*, 1991), even in nutrient conditions that do not naturally drive Rod1-GFP localization to the TGN (Figure 3A; Glc O/N and Lac, 4 h). Of note, Rod1-PH^{FAPP1}-GFP was more cytosolic in lactate medium than when glucose was present, probably because the TGN pool of PI(4)P is strongly influenced by glucose availability (Faulhammer *et al.*, 2005; Demmel *et al.*, 2008). Regardless, Rod1-PH^{FAPP1}-GFP was more strongly associated to the TGN than endogenous Rod1-GFP upon glucose addition to lactate-grown cells (Figure 3A).

We then used this tool to evaluate the function of Rod1 at the TGN using Jen1 degradation as a proxy. The expression of Rod1-PH^{FAPP1} restored Jen1 degradation in a *rod1*Δ background as efficiently as Rod1 (Figure 3, B and C). We hypothesized that this was only possible because endogenous Bul1 may compensate for the loss of Rod1 function at the plasma membrane. Although Rod1-PH^{FAPP1} expression in a *rod1*Δ *bul1*Δ background partially restored Jen1 degradation, in line with the importance of TGN-based sorting in this process, it was significantly less efficient than WT Rod1 to do so (Figure 3, B and C). Thus, a stronger association of Rod1 to the TGN leads to an increased dependency toward the function of Bul1 for Jen1 degradation. This supports the idea that multiple Rsp5 adaptors sequentially act at several subcellular locations during transporter endocytosis.

Bul1 phosphorylation is regulated by glucose availability

Several ARTs are targeted by nutrient-signaling kinases/phosphatases (O'Donnell *et al.*, 2010, 2013, 2015; MacGurn *et al.*, 2011; Becuwe *et al.*, 2012b; Merhi and André, 2012; Llopis-Torregrosa *et al.*, 2016; Hovsepian *et al.*, 2017). In particular, nitrogen availability

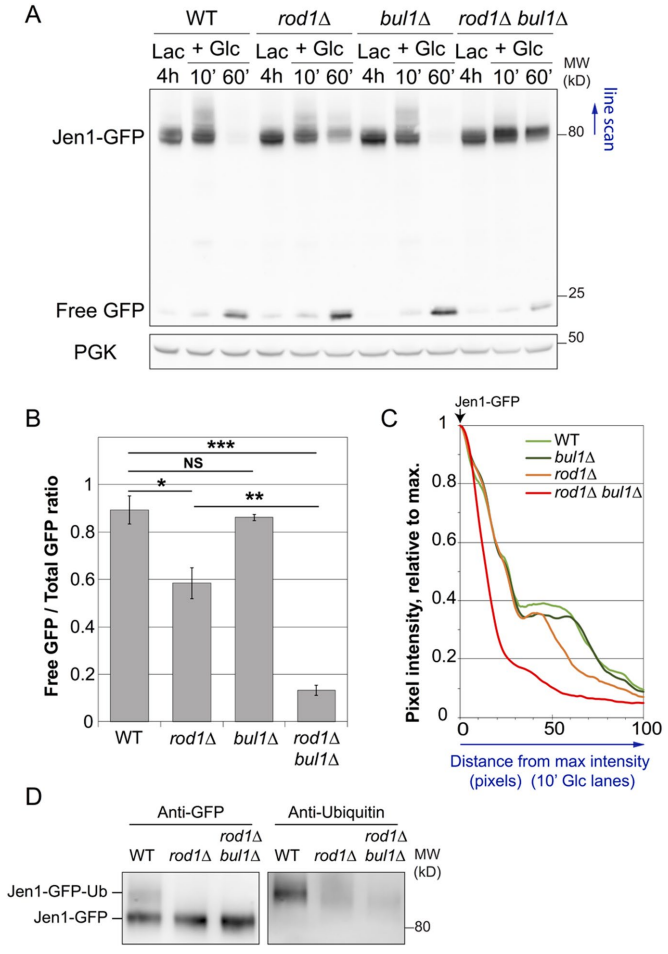

FIGURE 2: Bul1 is responsible for the residual ubiquitylation and degradation of Jen1 observed in the *rod1*Δ strain. (A) Degradation of Jen1-GFP over time after glucose treatment in WT, *rod1*Δ, *bul1*Δ, and *rod1*Δ *bul1*Δ cells. Total protein extracts were analyzed by SDS–PAGE and Western blotting using the indicated antibodies. PGK: phosphoglycerate kinase (loading control). (B) Quantification of the degradation of Jen1-GFP for each strain (ratio of free GFP over total GFP signal at the 60 min time point; see *Materials and Methods*). (C) Line scan of the Western blot presented in A showing pixel intensity (relative to the max intensity for each lane) over 100 pixels. (D) Jen1-GFP was immunopurified in denaturing conditions from the indicated strains, 10 min after glucose treatment. Immunoprecipitates were blotted with anti-GFP and anti-ubiquitin antibodies.

regulates Bul1/2 phosphorylation through a balanced activity of the TORC1-regulated kinase Npr1 and Sit4, a type 2A–related protein phosphatase. This allows Gap1 endocytosis to occur only when a rich N source is present in the medium (Merhi and André, 2012). So, we investigated whether Bul1 posttranslational modifications also responded to glucose availability.

In protein extracts from glucose-grown cells, Bul1-Flag migrated as a doublet (Figure 4A) much like what is observed in ammonium-treated cells (Merhi and André, 2012), in which Bul1 is ubiquitylated. Mutation of the Rsp5-binding motifs on Bul1 (Bul1-PYm), which abrogates Bul1 ubiquitylation (Merhi and André, 2012), led to a disappearance of the slower-migrating species of Bul1, revealing that it corresponded to ubiquitylated species (Figure 4, A and B). Here, we always used ammonium as a nitrogen source; this could explain why Bul1 was constitutively ubiquitylated in our conditions. However, we noticed a decreased mobility of Bul1-Flag species (both ubiquitylated and nonubiquitylated forms) when cells were grown in lactate medium. Treatment of these samples with alkaline phosphatase demonstrated that this was due to Bul1 phosphorylation (Figure 4, C and D). Thus, Bul1 is phosphorylated in the absence of glucose and dephosphorylated upon glucose addition, establishing Bul1 as a new glucose-responsive adaptor.

We previously reported that the glucose-induced dephosphorylation of Rod1 coincides with a change in its subcellular localization (Becuwe and Leon, 2014). Unfortunately, we were not able to study Bul1 localization because GFP-tagged versions of Bul1 were not functional (unpublished data).

The glucose-induced dephosphorylation of Bul1 requires Sit4

The PP1 phosphatase Glc7^{Reg1} is required for Rod1 dephosphorylation in response to glucose (Becuwe *et al.*, 2012b); however, in a *reg1*Δ mutant, Bul1 dephosphorylation still occurred (Figure 5A) suggesting the involvement of another phosphatase. Previous work indicated that Sit4 regulates Snf1 phosphorylation (Bozaquel-Morais *et al.*, 2010) and acts redundantly with Glc7^{Reg1} for Snf1 dephosphorylation when glucose levels are restored (Ruiz *et al.*, 2011). Because Sit4 is also required for Bul1 dephosphorylation in response to ammonium (Merhi and André, 2012), we tested its involvement in the glucose-induced dephosphorylation of Bul1. Indeed, Sit4 contributed to this regulation because Bul1 remained partially phosphorylated after glucose treatment in the *sit4*Δ mutant (Figure 5, B and C).

We then studied the potential involvement of Sit4 in Jen1 endocytosis. For this experiment, we used a galactose-inducible version of Jen1 (Paiva *et al.*, 2009) because endogenous Jen1 was not expressed in the *sit4*Δ mutant (unpublished data). In *sit4*Δ cells, Jen1 was endocytosed in response to glucose similarly to the WT (Figure 5, D and E). However, the deletion of *SIT4* in the *rod1*Δ mutant increased the endocytosis defect observed in the single *rod1*Δ mutant. Although this could be indirect, this reminds one of the situation observed with Bul1, which is not required per se for endocytosis, but becomes important when Rod1 is absent.

Bul1 is also required for the cycloheximide-induced endocytosis of Jen1

Bul1/Bul2, as targets of the TORC1-regulated kinase Npr1, are ideal players of nitrogen-regulated endocytosis (Helliwell *et al.*, 2001; Soetens *et al.*, 2001; Merhi and André, 2012). Interestingly, Jen1 is also endocytosed upon cycloheximide (CHX) treatment (Becuwe *et al.*, 2012b), a condition used to trigger transporter endocytosis in a Npr1-dependent manner (MacGurn *et al.*, 2011). Jen1 endocytosis after CHX treatment occurred independently of Rod1, but the deletion of *BUL1* strongly interfered with this process, and with no additional effect of the deletion of *ROD1* (Figure 5, F and G). Thus, Jen1 is an endocytic cargo for Bul1 after CHX treatment. If glucose indeed relieves Bul1 of its phosphoinhibition through its Sit4-dependent dephosphorylation, and because Bul1 is activated similarly in the presence of rich N sources, this may explain why Bul1 targets Jen1 both after glucose and CHX treatment. These results are in line with a recently published paper in which Bul1 was found to participate in Jen1 endocytosis in response to CHX, independently of Rod1 (Talaia *et al.*, 2017).

In conclusion, whereas the most essential function of Rod1 in Jen1 trafficking in response to glucose occurs at the TGN, Bul1 acts primarily at the plasma membrane. This sequential action of ARTs may allow a fine-tuning of transporter trafficking with respect to the

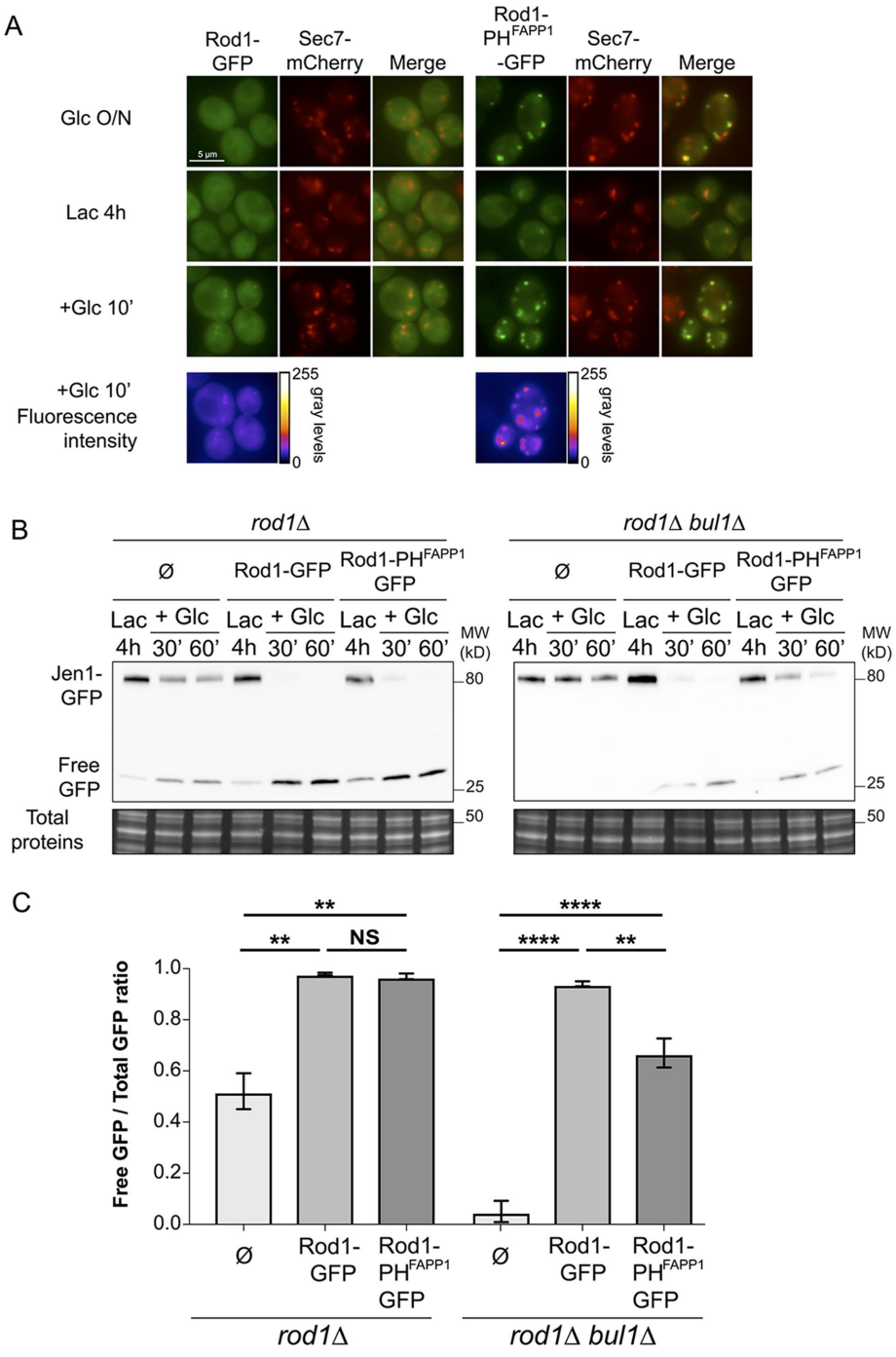

FIGURE 3: Expression of a TGN-localized version of Rod1 leads to an increased dependency toward the function of Bul1 for Jen1 degradation. (A) Localization of Rod1-GFP and Rod1-PH^{FAPP1}-GFP in wild-type yeast cells expressing the TGN marker, Sec7-mCherry, in the indicated culture conditions. Bottom, false-color images of the 10 min Glc time point showing increased TGN association of Rod1-PH^{FAPP1}-GFP over Rod1-GFP (generated using the "Fire" lookup table in ImageJ). (B) Degradation of Jen1-GFP over time after glucose treatment in *rod1*Δ or *rod1*Δ *bul1*Δ cells, carrying an empty plasmid or plasmids encoding Rod1-PH^{FAPP1}-GFP or Rod1-GFP. Note that both Rod1/Rod1-PH^{FAPP1} and Jen1 are tagged with GFP; however, Rod1/Rod1-PH^{FAPP1} are expressed at a much lower level (8- to 16-fold less than Jen1, respectively; see Supplemental Figure S2) and do not interfere with the detection of Jen1-GFP signals. (C) Quantification of Jen1-GFP degradation for each strain (60 min time point; see *Materials and Methods*).

cell's physiology. Additionally, our data may also provide a rationale for the functional redundancy in the ART family that was pointed out very early on (Lin *et al.*, 2008; Nikko *et al.*, 2008; Nikko and Pelham, 2009). We show that the Sit4-dependent Bul1 dephosphorylation, a prerequisite for its activation during ammonium-induced endocytosis of Gap1 (Merhi and André, 2012), also occurs after glucose treatment. Sit4 also regulates phosphorylation of Snf1, suggesting that its activity may be stimulated by glucose (Bozaquel-Morais *et al.*, 2010; Ruiz *et al.*, 2012). Thus, independent signals (glucose or nitrogen) may converge onto Sit4 to promote Bul1 dephosphorylation and possibly, its activation. It was possible that Bul1 only substitutes for Rod1 during glucose-induced endocytosis because of the void created by the absence of Rod1. To test this hypothesis, we expressed an inactive mutant version of Rod1, Rod1-PYm (which no longer interacts with Rsp5) and tested whether this would prevent Bul1 function, that is, whether this would phenocopy the *rod1*Δ *bul1*Δ double deletion. The results indicate that this is not the case (Supplemental Figure S3), suggesting that Bul1 is still active despite the expression of Rod1-PYm. This is in line with our previous results using an inactive, nonubiquitylatable Rod1-KR mutant that failed to restore Jen1 degradation when expressed in a *rod1*Δ mutant but did not aggravate the trafficking defect (Becuwe *et al.*, 2012b). Regardless of whether Bul1 acts only in the context of the *rod1*Δ mutant or also contributes to endocytosis in a WT context, Bul1 might be able to do so because 1) Jen1 is a target of Bul1 in other conditions (e.g., endocytosis in response to CHX, or other signals; Talaia *et al.*, 2017) and 2) Bul1 can be activated by glucose. We propose that the multiplicity of actors involved in signaling pathways that are solicited upon a given nutrient change may translate into multiple ART activations and redundancy, and ultimately contribute to an increased robustness in the adaptive response.

MATERIALS AND METHODS

Yeast strains, transformation, and growth conditions

Strains are listed by occurrence in each figure in Supplemental Table 1. Supplemental Table 2 describes their full genotype and references**.** All strains are derivatives of the BY4741 strains. Yeast was transformed by standard lithium acetate/polyethylene glycol procedure. Cells were grown in synthetic complete (SC) medium containing 2% (wt/vol) glucose or 0.5% (vol/vol) Na-lactate (pH 5.0; Sigma). For lactate inductions, cells were grown overnight in SC-glucose medium, harvested in early exponential phase (A_{600} = 0.3), resuspended in the same volume of SC-lactate medium, and grown for 4 h (A_{600} = 0.5) before the addition of glucose (2% wt/vol, final

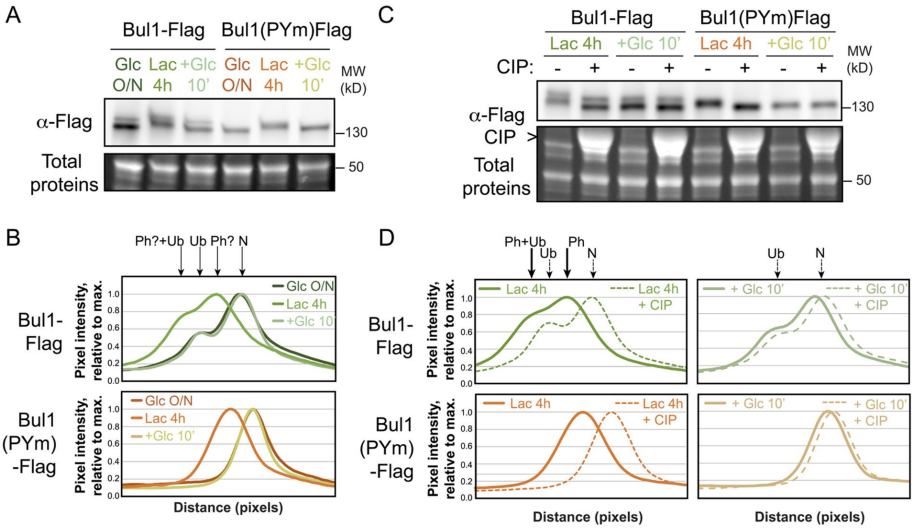

FIGURE 4: Glucose regulates Bul1 phosphorylation. (A) Western blot from total protein extracts prepared from cells expressing ether Bul1-Flag or Bul1(PYm)-Flag and grown as indicated. (B) Line scan of the Western blot presented in A showing pixel intensity (relative to the max intensity for each lane) over 100 pixels. (C) Western blot on total protein extracts prepared from cells expressing ether Bul1-Flag or Bul1(PYm)-Flag and grown as indicated, and treated or not with calf intestinal phosphatase (CIP). (D) Line scan of the Western blot presented in C.

concentration) or CHX (100 µg/ml) for the indicated time. For galactose induction, cells were precultured in SC-glucose medium, and grown overnight to early exponential phase (A_{600} = 0.3) in SC medium containing 2% raffinose (wt/vol) and 0.02% glucose (wt/vol) to initiate growth. Galactose was then added at a final concentration of 2% (wt/vol), and cells were grown for 2 h. Chase and endocytosis were both initiated by adding glucose to a final concentration of 2% (wt/vol) and incubating for the indicated times. For Figure 1E, cells were incubated for 5 min at 30°C with latrunculin A (Sigma; final concentration: 0.2 mM) before glucose addition.

Plasmids

The plasmids used in this study are listed in Supplemental Table 3. Plasmids pMA121 (YCp-*BUL1*-FLAG; *URA3*) and pMA136 (YCp-*BUL1[PYm]*-FLAG; *URA3*) were a kind gift from Bruno André, Université Libre de Bruxelles, Gosselies, Belgium (Merhi and André, 2012). For the Rod1-PH^{FAPP1}-GFP plasmid (pSL164; p_{ROD1}:Rod1-PH^{FAPP1}-GFP), the FAPP1 sequence (a kind gift from Chris Stefan, MRC Laboratory for Molecular Cell Biology, University College London, UK, and Catherine Jackson, Institut Jacques Monod, Paris, France) was amplified by PCR (using primers oSL349/oSL350, *Xma*I/*Xma*I) and cloned at the *Xma*I site into pSL93 (p416-based, *pROD1*:Rod1-GFP; Becuwe *et al.*, 2012b). Orientation was checked by restriction digest and sequencing.

Note that the tagged proteins used in this article were functional: Bul1-Flag was able to restore ammonium-induced endocytosis of Gap1 when expressed in a *bul1*Δ *bul2*Δ strain (Merhi and André, 2012), Jen1-GFP was shown to be functional for lactate uptake (Paiva *et al.*, 2009), and Rod1-GFP is functional because it restored Jen1 endocytosis in the context of both the *rod1*Δ and the *rod1*Δ *bul1*Δ mutants (Figure 3B).

Total protein extracts and phosphatase treatment

For total protein extracts, trichloroacetic acid (TCA; Sigma) was added directly in the culture to a final concentration of 10% (vol/vol), and cells were precipitated on ice for 10 min. Cells were then harvested by centrifugation for 1 min at room temperature at 16,000 × *g*, resuspended in 100 µl of TCA (10%, vol/vol), and lysed with glass beads for 10 min at 4°C. Beads were removed, the lysate was centrifuged for 1 min at room temperature at 16,000 × *g*, and the resulting pellet was resuspended in TCA-sample buffer (Tris-HCl 50 mM, pH 6.8, dithiothreitol 100 mM, SDS 2%, bromphenol blue 0.1%, glycerol 10%, containing 200 mM of unbuffered Tris solution) at a concentration of 50 µl/initial OD unit, before being denatured at 37°C for 10 min in a thermomixer (1400 rpm). Samples (10 µl) were loaded on SDS–PAGE gel. Phosphatase treatment was performed as previously described (Becuwe *et al.*, 2012b).

Immunoprecipitation of Jen1-GFP in denaturing conditions

To immunoprecipitate Jen1-GFP, 50 OD equivalents of yeast cells grown for 4 h in lactate medium and treated with 2% glucose for 10 min were used. Yeast cells were mechanically disrupted with glass beads using a vortex at 4°C in 500 µl ice-cold RIPA lysis buffer (50 mM Tris-HCl, pH 7.5, 150 mM NaCl, 0.1% SDS, 2 mM EDTA, 50 mM NaF, 1% NP-40, 0.5% Na-deoxycholate [Sigma-Aldrich], 1% glycerol) containing protease inhibitors (cOmplete Protease Inhibitor Cocktail [Roche Life Sciences], 2 mM phenylmethylsulfonyl fluoride [Sigma-Aldrich], and 20 mM NEM [*N*-ethylmaleimide; Sigma-Aldrich]) using four cycles of lysis (2 min), each separated by 2 min on ice. The lysate was then gently incubated on rotation on a wheel for 30 min at 4°C for solubilization. Then, 500 µl of wash buffer (50 mM Tris-HCl, pH 7.5, 150 mM NaCl, 1% NP-40, 5% glycerol, containing 20 mM NEM) was added and the sample was vortexed to mix and further rotated for 1 h at 4°C for better solubilization. After vortexing for 3 min, the lysate was centrifuged at 10,000 × *g* for 10 min at 4°C. The cleared lysate (supernatant) was then transferred to another tube, to which were added 10 µl of GFP-Trap_MA magnetic agarose beads (ChromoTek GmbH, Planegg-Martinsried, Germany) prewashed twice in 1 ml of wash buffer. The sample was rotated overnight at 4°C. The beads were then collected using a magnetic rack and washed twice by rotating for 15 min at 4°C with 1.5 ml ice-cold wash buffer. The beads were further washed for 30 min at room temperature with 1.5 ml Tris-buffered saline buffer (50 mM Tris-HCl, pH 7.5, 150 mM NaCl), containing 0.1% Tween 20. The beads were then collected and resuspended in 50 µl of 2× urea sample buffer (150 mM Tris-HCl, pH 6.8, 6M urea, 6% SDS, 0.01% bromphenol blue) and then incubated for 30 min at 37°C in a thermomixer (1400 rpm). Then, 50 µl of boiling buffer (50 mM Tris-HCl, pH 7.5, 1 mM EDTA, 1% SDS, 20% glycerol) was added and the sample was further incubated for 1 h at 37°C in a thermomixer (1400 rpm).

Antibodies, immunoblotting, and quantifications

We used monoclonal antibodies raised against GFP (clones 7.1 and 13.1; cat #11814460001; Roche Life Sciences, Meyland, France), Flag (clone M2, ref. F1804; Sigma), anti-ubiquitin (clone P4D1, ref. sc-8017; Santa Cruz Biotechnology, Dallas, TX), and rabbit polyclonal antibodies against 3-phosphoglycerate kinase (PGK, ref. NE130/7S; Nordic-MUbio BV, Susteren, Netherlands). Horseradish peroxidase–coupled secondary antibodies were from Sigma (anti-mouse, ref A5278; anti-rabbit, ref. A6154). Chemiluminescence signals were

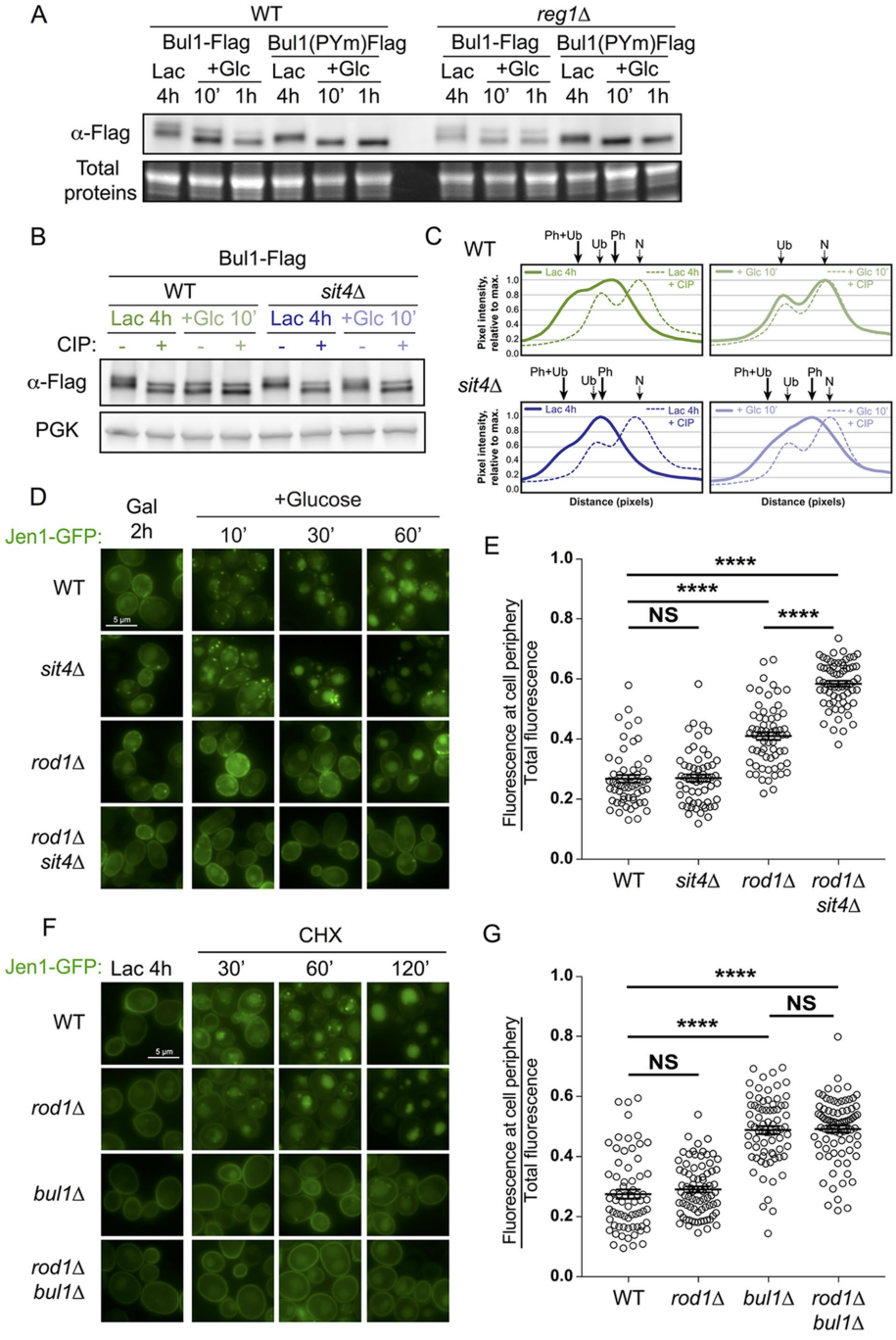

FIGURE 5: The glucose-induced dephosphorylation of Bul1 requires Sit4. (A) Western blot from total protein extracts prepared from WT or *reg1*Δ cells expressing either Bul1-Flag or Bul1(PYm)-Flag and grown as indicated. (B) Western blot from total protein extracts prepared from WT or *sit4*Δ cells expressing Bul1-Flag grown as indicated and treated or not with calf intestinal phosphatase (CIP). (C) Line scan of the Western blot presented in B. (D) Localization of a galactose-inducible Jen1-GFP in WT, *sit4*Δ, *rod1*Δ, and *rod1*Δ *sit4*Δ cells after galactose induction or at various times after glucose treatment. (E) From the experiment presented in D, quantification of the ratio of fluorescence at the cell periphery over total fluorescence. (F) Localization of Jen1-GFP in WT, *rod1*Δ, *bul1*Δ, and *rod1*Δ *bul1*Δ cells after lactate induction or various times after CHX treatment. (G) From the experiment presented in H, quantification of the ratio of fluorescence at the cell periphery over total fluorescence.

acquired with the LAS-4000 imaging system (Fuji, Tokyo, Japan). Quantifications were performed using ImageJ (National Institutes of Health) on nonsaturated blots from independent experiments ($n \geq 3$).

For Figures 2B and 3C, the ratio of the free GFP signal over the total GFP signal was calculated for the 60 min time point ($n = 3$ biological replicates). An unpaired, two-sided *t* test was performed using Prism 7.0 (GraphPad software, La Jolla, CA) and the *p* values are indicated (NS: $p > 0.05$; *, $p < 0.05$; **, $p < 0.01$; ***, $p < 0.001$; ****, $p < 0.0001$). For line scans (Figures 2C, 4, B and D, and 5C), a line was drawn in the center of the lane, along the area of interest, and the intensity profile was plotted. Lanes were aligned with each other to correct for potential heterogeneity in the migration using a reference band present in all lanes.

In all figures except Figure 2, total proteins were visualized in gels using a trihalo compound incorporated in SDS–PAGE gels (stain-free TGX gels, 4–20%; Bio-Rad) after 1 min UV-induced photoactivation and imaging using a Gel Doc EZ Imager (Bio-Rad). In Figure 2, samples were loaded on SDS–PAGE 4–12% gels (Bis-Tris) from Invitrogen that we found more suitable for ubiquitin visualization.

Fluorescence microscopy and quantifications

Cells were mounted in the appropriate culture medium and imaged at room temperature with a motorized Olympus BX-61 fluorescence microscope equipped with an Olympus PlanApo 100× oil-immersion objective (1.40 NA), a QiClick cooled monochrome camera (QImaging, Surrey, BC, Canada), and the MetaVue acquisition software (Molecular Devices, Sunnyvale, CA). GFP-tagged proteins were visualized using a GFP filter set (41020 from Chroma Technology, Bellows Falls, VT; excitation HQ480/20×, dichroic Q505LP, emission HQ535/50m). mCherry-tagged proteins were visualized using an HcRedI filter set (41043 from Chroma Technology, Bellows Falls, VT; excitation HQ575/50×, dichroic Q610lp, emission HQ640/50m). Vacuolar staining was obtained by incubating cells with 100 μM CMAC (7-amino-4-chloromethylcoumarin; ThermoFisher) for 10 min under agitation at 30°C; cells were then washed twice with the appropriate medium and observed with a DAPI (4′, 6-diamidino-2-phenylindole) filter set (31013v2; Chroma Technology Corp.; excitation D365/10×, dichroic 400DCLP, emission D460/50m). Images were processed in ImageJ for levels and for contrast when indicated.

For quantification of intracellular/peripheral fluorescence signals, a first ellipse was drawn around each cell ($n > 50$ cells) using ImageJ, and a second ellipse was drawn inside the cell so as to exclude the plasma-membrane localized signal. The integrated density (IntDens) of both

of these regions of interest were measured, to which the background noise for each ellipse was subtracted, giving a corrected value of IntDens (IntDensCorr). Background noise was calculated by multiplying the area of the ellipse of interest by the average gray value per pixel as measured in a control region. The difference (IntDensCorr[1st ellipse]–IntDensCorr[2nd ellipse]) was taken as a value of the peripheral (plasma membrane) signal**.** An unpaired, two-tailed *t* test was performed using Prism 7.0 (GraphPad Software; La Jolla, CA), and the *p* values are indicated (NS: $p > 0.05$; *, $p < 0.05$; **, $p < 0.01$; ***, $p < 0.001$; ****, $p < 0.0001$).

ACKNOWLEDGMENTS

We thank Bruno André (Université libre de Bruxelles, Brussels, Belgium), Catherine Jackson (Institut Jacques Monod, Paris, France), and Chris Stefan (MRC Laboratory for Molecular Cell Biology, University College, London, UK) for providing reagents. This work was supported by the Ligue contre le Cancer (RS17/75-90 and RS18/75-81 to S.L.), the Agence Nationale pour la Recherche ("P-Nut," ANR-16-CE13-0002-01 to S.L. and D.T.), and the Austrian Science Fund (FWF-Y444-B12, P 29583) and MCBO (W1101-B18) to D.T. We also acknowledge the EU COST network BM1307 "Proteostasis" for networking opportunities.

REFERENCES

Abe F, Iida H (2003). Pressure-induced differential regulation of the two tryptophan permeases Tat1 and Tat2 by ubiquitin ligase Rsp5 and its binding proteins, Bul1 and Bul2. Mol Cell Biol 23, 7566–7584.

Alvaro CG, Aindow A, Thorner J (2016). Differential phosphorylation provides a switch to control how α-arrestin Rod1 down-regulates mating pheromone response in *Saccharomyces cerevisiae*. Genetics 203, 299–317.

Alvaro CG, O'Donnell AF, Prosser DC, Augustine AA, Goldman A, Brodsky JL, Cyert MS, Wendland B, Thorner J (2014). Specific α-arrestins negatively regulate *Saccharomyces cerevisiae* pheromone response by down-modulating the G-protein-coupled receptor Ste2. Mol Cell Biol 34, 2660–2681.

Becuwe M, Herrador A, Haguenauer-Tsapis R, Vincent O, Léon S (2012a). Ubiquitin-mediated regulation of endocytosis by proteins of the arrestin family. Biochem Res Int 2012, 242764.

Becuwe M, Leon S (2014). Integrated control of transporter endocytosis and recycling by the arrestin-related protein Rod1 and the ubiquitin ligase Rsp5. eLife 3, 03307.

Becuwe M, Vieira N, Lara D, Gomes-Rezende J, Soares-Cunha C, Casal M, Haguenauer-Tsapis R, Vincent O, Paiva S, Léon S (2012b). A molecular switch on an arrestin-like protein relays glucose signaling to transporter endocytosis. J Cell Biol 196, 247–259.

Bozaquel-Morais BL, Madeira JB, Maya-Monteiro CM, Masuda CA, Montero-Lomeli M (2010). A new fluorescence-based method identifies protein phosphatases regulating lipid droplet metabolism. PLoS One 5, e13692.

Broach JR (2012). Nutritional control of growth and development in yeast. Genetics 192, 73–105.

Chambers P, Issaka A, Palecek SP (2004). *Saccharomyces cerevisiae* JEN1 promoter activity is inversely related to concentration of repressing sugar. Appl Environ Microbiol 70, 8–17.

Conibear E, Stevens TH (2000). Vps52p, Vps53p, and Vps54p form a novel multisubunit complex required for protein sorting at the yeast late Golgi. Mol Biol Cell 11, 305–323.

Crapeau M, Merhi A, Andre B (2014). Stress conditions promote yeast Gap1 permease ubiquitylation and down-regulation via the arrestin-like Bul and Aly proteins. J Biol Chem 289, 22103–22116.

Demmel L, Beck M, Klose C, Schlaitz AL, Gloor Y, Hsu PP, Havlis J, Shevchenko A, Krause E, Kalaidzidis Y, Walch-Solimena C (2008). Nucleocytoplasmic shuttling of the Golgi phosphatidylinositol 4-kinase Pik1 is regulated by 14-3-3 proteins and coordinates Golgi function with cell growth. Mol Biol Cell 19, 1046–1061.

Dowler S, Currie RA, Campbell DG, Deak M, Kular G, Downes CP, Alessi DR (2000). Identification of pleckstrin-homology-domain-containing proteins with novel phosphoinositide-binding specificities. Biochem J 351, 19–31.

Faulhammer F, Konrad G, Brankatschk B, Tahirovic S, Knodler A, Mayinger P (2005). Cell growth-dependent coordination of lipid signaling and glycosylation is mediated by interactions between Sac1p and Dpm1p. J Cell Biol 168, 185–191.

Franzusoff A, Redding K, Crosby J, Fuller RS, Schekman R (1991). Localization of components involved in protein transport and processing through the yeast Golgi apparatus. J Cell Biol 112, 27–37.

Galan JM, Moreau V, André B, Volland C, Haguenauer-Tsapis R (1996). Ubiquitination mediated by the Npi1p/Rsp5p ubiquitin-protein ligase is required for endocytosis of the yeast uracil permease. J Biol Chem 271, 10946–10952.

Ghaddar K, Merhi A, Saliba E, Krammer EM, Prevost M, Andre B (2014). Substrate-induced ubiquitylation and endocytosis of yeast amino acid permeases. Mol Cell Biol 34, 4447–4463.

Gournas C, Amillis S, Vlanti A, Diallinas G (2010). Transport-dependent endocytosis and turnover of a uric acid-xanthine permease. Mol Microbiol 75, 246–260.

Guiney EL, Klecker T, Emr SD (2016). Identification of the endocytic sorting signal recognized by the Art1-Rsp5 ubiquitin ligase complex. Mol Biol Cell 27, 4043–4054.

Haguenauer-Tsapis R, André B (2004). Membrane trafficking of yeast transporters: mechanisms and physiological control of downregulation. Top Curr Genet 9, 273–323.

Hatakeyama R, Kamiya M, Takahara T, Maeda T (2010). Endocytosis of the aspartic acid/glutamic acid transporter Dip5 is triggered by substrate-dependent recruitment of the Rsp5 ubiquitin ligase via the arrestin-like protein Aly2. Mol Cell Biol 30, 5598–5607.

He J, Scott JL, Heroux A, Roy S, Lenoir M, Overduin M, Stahelin RV, Kutateladze TG (2011). Molecular basis of phosphatidylinositol 4-phosphate and ARF1 GTPase recognition by the FAPP1 pleckstrin homology (PH) domain. J Biol Chem 286, 18650–18657.

Hein C, Springael JY, Volland C, Haguenauer-Tsapis R, André B (1995). NPI1, an essential yeast gene involved in induced degradation of Gap1 and Fur4 permeases, encodes the Rsp5 ubiquitin-protein ligase. Mol Microbiol 18, 77–87.

Helliwell SB, Losko S, Kaiser CA (2001). Components of a ubiquitin ligase complex specify polyubiquitination and intracellular trafficking of the general amino acid permease. J Cell Biol 153, 649–662.

Hovsepian J, Defenouillere Q, Albanese V, Vachova L, Garcia C, Palkova Z, Leon S (2017). Multilevel regulation of an α-arrestin by glucose depletion controls hexose transporter endocytosis. J Cell Biol 216, 1811–1831.

Karachaliou M, Amillis S, Evangelinos M, Kokotos AC, Yalelis V, Diallinas G (2013). The arrestin-like protein ArtA is essential for ubiquitination and endocytosis of the UapA transporter in response to both broad-range and specific signals. Mol Microbiol 88, 301–317.

Keener JM, Babst M (2013). Quality control and substrate-dependent downregulation of the nutrient transporter Fur4. Traffic 14, 412–427.

Levine TP, Munro S (2002). Targeting of Golgi-specific pleckstrin homology domains involves both PtdIns 4-kinase-dependent and -independent components. Curr Biol 12, 695–704.

Lin CH, MacGurn JA, Chu T, Stefan CJ, Emr SD (2008). Arrestin-related ubiquitin-ligase adaptors regulate endocytosis and protein turnover at the cell surface. Cell 135, 714–725.

Liu J, Sitaram A, Burd CG (2007). Regulation of copper-dependent endocytosis and vacuolar degradation of the yeast copper transporter, Ctr1p, by the Rsp5 ubiquitin ligase. Traffic 8, 1375–1384.

Llopis-Torregrosa V, Ferri-Blazquez A, Adam-Artigues A, Deffontaines E, van Heusden GP, Yenush L (2016). Regulation of the yeast Hxt6 hexose transporter by the Rod1 α-arrestin, the Snf1 protein kinase, and the Bmh2 14-3-3 protein. J Biol Chem 291, 14973–14985.

Lodi T, Fontanesi F, Guiard B (2002). Co-ordinate regulation of lactate metabolism genes in yeast: the role of the lactate permease gene JEN1. Mol Genet Genomics 266, 838–847.

MacGurn JA, Hsu PC, Emr SD (2012). Ubiquitin and membrane protein turnover: from cradle to grave. Annu Rev Biochem 81, 231–259.

MacGurn JA, Hsu PC, Smolka MB, Emr SD (2011). TORC1 regulates endocytosis via Npr1-mediated phosphoinhibition of a ubiquitin ligase adaptor. Cell 147, 1104–1117.

McCracken AN, Edinger AL (2013). Nutrient transporters: the Achilles' heel of anabolism. Trends Endocrinol Metab 24, 200–208.

Merhi A, André B (2012). Internal amino acids promote Gap1 permease ubiquitylation via TORC1/Npr1/14-3-3-dependent control of the Bul arrestin-like adaptors. Mol Cell Biol 32, 4510–4522.

Mota S, Vieira N, Barbosa S, Delaveau T, Torchet C, Le Saux , A, Garcia , M, Pereira A, Lemoine S, Coulpier F, *et al*. (2014). Role of the DHH1 gene

in the regulation of monocarboxylic acids transporters expression in *Saccharomyces cerevisiae*. PLoS One 9, e111589.
Nikko E, Pelham HR (2009). Arrestin-mediated endocytosis of yeast plasma membrane transporters. Traffic 10, 1856–1867.
Nikko E, Sullivan JA, Pelham HR (2008). Arrestin-like proteins mediate ubiquitination and endocytosis of the yeast metal transporter Smf1. EMBO Rep 9, 1216–1221.
O'Donnell AF, Apffel A, Gardner RG, Cyert MS (2010). α-Arrestins Aly1 and Aly2 regulate intracellular trafficking in response to nutrient signaling. Mol Biol Cell 21, 3552–3566.
O'Donnell AF, Huang L, Thorner J, Cyert MS (2013). A calcineurin-dependent switch controls the trafficking function of α-arrestin Aly1/Art6. J Biol Chem 288, 24063–24080.
O'Donnell AF, McCartney RR, Chandrashekarappa DG, Zhang BB, Thorner J, Schmidt MC (2015). 2-Deoxyglucose impairs *Saccharomyces cerevisiae* growth by stimulating Snf1-regulated and α-arrestin-mediated trafficking of hexose transporters 1 and 3. Mol Cell Biol 35, 939–955.
Paiva S, Vieira N, Nondier I, Haguenauer-Tsapis R, Casal M, Urban-Grimal D (2009). Glucose-induced ubiquitylation and endocytosis of the yeast Jen1 transporter: role of lysine 63-linked ubiquitin chains. J Biol Chem 284, 19228–19236.
Piper RC, Dikic I, Lukacs GL (2014). Ubiquitin-dependent sorting in endocytosis. Cold Spring Harb Perspect Biol 6, doi: 10.1101/cshperspect.a016808.
Pizzirusso M, Chang A (2004). Ubiquitin-mediated targeting of a mutant plasma membrane ATPase, Pma1-7, to the endosomal/vacuolar system in yeast. Mol Biol Cell 15, 2401–2409.
Risinger AL, Kaiser CA (2008). Different ubiquitin signals act at the Golgi and plasma membrane to direct GAP1 trafficking. Mol Biol Cell 19, 2962–2972.
Rotin D, Kumar S (2009). Physiological functions of the HECT family of ubiquitin ligases. Nat Rev Mol Cell Biol 10, 398–409.
Ruiz A, Liu Y, Xu X, Carlson M (2012). Heterotrimer-independent regulation of activation-loop phosphorylation of Snf1 protein kinase involves two protein phosphatases. Proc Natl Acad Sci USA 109, 8652–8657.
Ruiz A, Xu X, Carlson M (2011). Roles of two protein phosphatases, Reg1-Glc7 and Sit4, and glycogen synthesis in regulation of SNF1 protein kinase. Proc Natl Acad Sci USA 108, 6349–6354.
Shinoda J, Kikuchi Y (2007). Rod1, an arrestin-related protein, is phosphorylated by Snf1-kinase in *Saccharomyces cerevisiae*. Biochem Biophys Res Commun 364, 258–263.
Sigismund S, Confalonieri S, Ciliberto A, Polo S, Scita G, Di Fiore PP (2012). Endocytosis and signaling: cell logistics shape the eukaryotic cell plan. Physiol Rev 92, 273–366.
Siniossoglou S, Pelham HR (2001). An effector of Ypt6p binds the SNARE Tlg1p and mediates selective fusion of vesicles with late Golgi membranes. EMBO J 20, 5991–5998.
Soetens O, De Craene JO, André B (2001). Ubiquitin is required for sorting to the vacuole of the yeast general amino acid permease, Gap1. J Biol Chem 276, 43949–43957.
Talaia G, Gournas C, Saliba E, Barata-Antunes C, Casal M, Andre B, Diallinas G, Paiva S (2017). The α-arrestin Bul1p mediates lactate transporter endocytosis in response to alkalinization and distinct physiological signals. J Mol Biol 429, 3678–3695.
Villers J, Savocco J, Szopinska A, Degand H, Nootens S, Morsomme P (2017). Study of the plasma membrane proteome dynamics reveals novel targets of nitrogen regulation in yeast. Mol Cell Proteomics 16, 1652–1668.
Zhao Y, Macgurn JA, Liu M, Emr S (2013). The ART-Rsp5 ubiquitin ligase network comprises a plasma membrane quality control system that protects yeast cells from proteotoxic stress. eLife 2, e00459.